



Delft University of Technology

System NEP Verification of a Wideband THz Direct Detector in CMOS

van Berkel, S.L.; Malotaux, E.S.; de Martino, C.; Spirito, M.; Cavallo, D.; Neto, A.; Llombart, N.

DOI

[10.1109/IRMMW-THz46771.2020.9370624](https://doi.org/10.1109/IRMMW-THz46771.2020.9370624)

Publication date

2020

Document Version

Final published version

Published in

2020 45th International Conference on Infrared, Millimeter, and Terahertz Waves, IRMMW-THz 2020

Citation (APA)

van Berkel, S. L., Malotaux, E. S., de Martino, C., Spirito, M., Cavallo, D., Neto, A., & Llombart, N. (2020). System NEP Verification of a Wideband THz Direct Detector in CMOS. In *2020 45th International Conference on Infrared, Millimeter, and Terahertz Waves, IRMMW-THz 2020* (pp. 72). Article 9370624 (International Conference on Infrared, Millimeter, and Terahertz Waves, IRMMW-THz; Vol. 2020-November). <https://doi.org/10.1109/IRMMW-THz46771.2020.9370624>

Important note

To cite this publication, please use the final published version (if applicable).

Please check the document version above.

Copyright

Other than for strictly personal use, it is not permitted to download, forward or distribute the text or part of it, without the consent of the author(s) and/or copyright holder(s), unless the work is under an open content license such as Creative Commons.

Takedown policy

Please contact us and provide details if you believe this document breaches copyrights.

We will remove access to the work immediately and investigate your claim.

System NEP Verification of a Wideband THz Direct Detector in CMOS

S.L. van Berkel¹, E.S. Malotaux², C. de Martino², M. Spirito², D. Cavallo¹, A. Neto¹, and N. Llombart¹

¹Delft University of Technology, Department of Microelectronics, Delft, The Netherlands

²Electronics Research Laboratory, Department of Microelectronics, Delft University of Technology, Delft, The Netherlands

Abstract— The predicted Noise Equivalent Power (NEP) of a THz direct detector is validated by means of a noise- and a system responsivity measurement. The direct detector consists of a double leaky slot lens antenna that operates from 200 GHz to 600 GHz in combination with a differential pair of Schottky Barrier Diodes (SBDs). The model is derived from low-frequency measurements.

I. INTRODUCTION AND BACKGROUND

Hz imaging applications are not yet widespread deployed mainly due to the size and cost of THz sources [1]. Future passive imaging applications, that would enable low-cost applications, require hundreds GHz of bandwidth together with low-noise detectors [2]. An accurate prediction of system NEP is required to push the performance in technologies such as CMOS. The Signal-to-Noise ratio of a direct detection system, after τ_{int} detector integration time can be written spectrally as:

$$\text{SNR}_{\text{AD}} = \frac{\sqrt{2\tau_{\text{int}}}}{\Delta f_{\text{RF}}} \int_{\Delta f_{\text{RF}}} \frac{p_{\text{sig}}(f)}{\text{NEP}_{\text{sys}}(f)} df$$

where Δf_{RF} is the bandwidth, $p_{\text{sig}}(f)$ is the power available to the antenna and NEP_{sys} is the system NEP that is defined as:

$$\text{NEP}_{\text{sys}} = \frac{v_n}{\mathfrak{R}_v^{\text{sys}}(f)} = \frac{v_n}{\mathfrak{R}_v^{\text{det}}(f) \eta_{\text{ant}}(f) \eta_{\Omega}(f)}$$

where, v_n is the spectral noise voltage, $\mathfrak{R}_v^{\text{sys}}$ and $\mathfrak{R}_v^{\text{det}}$ are the voltage responsivity of the system or detection circuit, η_{ant} is the antenna efficiency and η_{Ω} is the impedance matching efficiency of the antenna-detector combination. An accurate prediction of the system performance requires a wideband modeling of the antenna, detection circuit and interface.

THZ DIRECT DETECTOR

As demonstrator for accurate wideband NEP modelling, the THz direct detector shown in Fig. 1(a) is considered. A 7.6 mm diameter elliptical lens is glued to a CMOS chip that contains a double leaky-slot antenna, operating from 200 GHz to 600 GHz with an average efficiency of $\bar{\eta}_{\text{ant}} = 57\%$ over the full bandwidth. In [3] the authors present the measured gain patterns of a similar antenna that is fabricated in a different CMOS technology. The detection circuit, as illustrated in Fig. 1(b) is a differential pair of SBDs which are connected to a load resistor of $2 \text{ k}\Omega$ for a voltage read-out. A reference branch is added for external noise rejection and enables a pseudo-differential read-out. The performance of the differential detection circuit, in terms of voltage responsivity $\mathfrak{R}_v^{\text{det}}$, can accurately be predicted by using the lumped element model of the SBD, shown in Fig. 1(c) [4,5]. The SBDs used in the THz direct detector are the smallest one that is provided by the process design kit of the technology ($1.6 \times 1.6 \mu\text{m}^2$) and its lumped element model, Fig. 1(c), is constructed from the measured IV-curve and S-parameters at 10 GHz. The dominant noise contributions, beyond the Flicker-noise corner, are the shot-noise generated in the junction of the SBDs and thermal (Johnson) noise of the

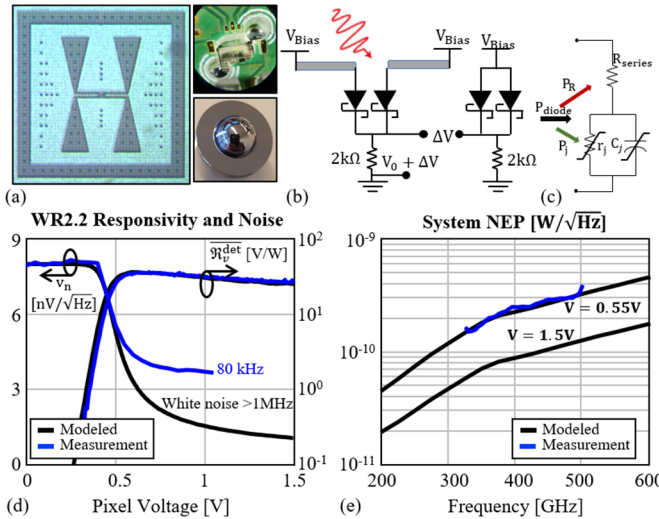


Fig. 1. THz Direct detector and measurements. (a) Double leaky-slot antenna , elliptical lens, and bondwiring to PCB. (b) Differential detection architecture. (c) Equivalent SBD Model. (d) Responsivity and noise averaged in the WR2.2 band. (e) Single ended NEP_{svs}.

load resistor and can be analytically predicted from the IV-curve and the dc equivalent circuit of the detection architecture.

SYSTEM MEASUREMENTS

The voltage responsivity of the THz direct detector $\mathfrak{R}_v^{\text{sys}}$ is measured in the WR2.2 frequency band, from 325 GHz to 500 GHz, using a VDI frequency extender connected to a horn antenna and by using a 60dB voltage gain amplifier (VGA). The detector voltage responsivity, $\mathfrak{R}_v^{\text{det}}$, deembedded by using the predicted antenna and matching efficiency, is shown in Fig. 1(d) and is compared with the model. The spectral noise voltage is measured using the VGA that is connected to a dynamic signal analyser (DSA) and is also shown in Fig. 1(d). The measurement, limited to the cut-off frequency of the VGA and DSA of 100 kHz, is performed at 80 kHz where the Flicker-noise is still dominant for higher biasing voltages. Flicker-noise is not included in the model and therefore deviates from the measurement. The spectral NEP at $V = 0.55\text{V}$, calculated from the measured system responsivity and spectral noise is shown in Fig. 1(e) and shows excellent agreement with the model. The modelled optimal NEP, at $V = 1.5\text{V}$ is also shown.

An accurate wideband prediction of system NEP is crucial for realizing future passive imaging applications that require hundreds GHz of bandwidth together with a $1 \text{ pW}/\sqrt{\text{Hz}}$ NEP.

REFERENCES

- [1] P. Hillger, et.al., "Terahertz Imaging and Sensing Applications with Silicon-Based Technologies," IEEE TTST, Dec. 2018.
- [2] S. van Berkel, et.al., "THz imaging using uncooled wideband direct detection focal plane arrays," IEEE TTST, 2017.
- [3] S. van Berkel, et.al., "Optical performance of a wideband 28nm CMOS double bow-tie slot antenna for imaging applications," in IRMMW, 2018.
- [4] R. Han, et.al., "A 280-GHz Schottky diode detector in 130-nm digital CMOS," IEEE JSSC, Nov. 2011.
- [5] A. M. Cowley and H. O. Sorensen, "Quantitative comparison of Solid-State microwave detectors," IEEE MTT, 1966.